Influential Synoptic Weather Types for a Future Renewable Energy Dependent National Electricity Market

Robert Huva, Roger Dargaville and Peter Rayner

School of Earth Sciences, University of Melbourne, Melbourne, Australia

This study presents an analysis of the synoptic scale influences on potential renewable energy output for eastern Australia (the National Electricity Market (NEM) region). Common synoptic scale weather patterns are identified using a Self-Organising Map (SOM) of 1989-2009 ERA-Interim Mean Sea-Level Pressure (MSLP) for the Australian region. Using wind speed and surface shortwave radiation output from the Australian Community Climate and Earth-System Simulator (ACCESS) regional model (ACCESS-R) for 2010-2011, in tandem with a Genetic Algorithm, a cost-optimal placement of renewable resources for the NEM is derived. Moments of very low output from the combination of wind and solar are then analysed to show that a ridging high pressure system south of Perth and a summer continental heat low significantly co-occur with very low output. Another MSLP type represented by a cold front approaching South Australia was shown to never associate with very low output. An investigation into the 2010-2011 period when compared to the previous 21 years showed that the La Niña conditions during 2010-2011 period were more challenging than normal for wind and solar for some areas. What the study also shows is that despite the large geographical area the NEM region cannot rely solely on non-dispatchable renewable electricity, without installing unrealistic amounts of over-capacity.

Introduction

In the context of Australia, research in recent years is starting to demonstrate that a large reliance on renewable energy, perhaps even 100 %, could be possible in the future without compromising supply to the network. Using data from the Bureau of Meteorology Wright and Hearps (2010) have shown that a mixture of 38 % concentrating solar thermal, 44 % wind power and 18 % other back-up sources, spread-out across the continent, could supply all of Australia's power needs by 2020. Elliston et al. (2013), which used Bureau of Meteorology and Australian Electricity Market Operator data, suggested the mix for a future 100 % renewable Australia could be between 46-58 % onshore wind power, 13-22 % concentrating solar thermal, 15-20 % photovoltaics, 5-6 % hydro and the remaining 5-6 % gas (fuelled by biofuels), depending on the cost assumptions. AEMO (2013) showed that Australian demand for electricity could be met in the year 2030 by a combination of 20-40 % of installed capacity from photovoltaics, 7-35 % onshore wind, 10-15 % concentrating solar thermal, 10-15 % biogas and then smaller amounts of capacity from other back-up resources (including hydro, geothermal and biomass). Importantly, both the AEMO (2013) and Elliston et al. (2013) studies were able to maintain the existing reliability requirements of only 0.002 % unserved energy per year.

To ensure demand is met by renewable electricity and minimise the influence of minima in one particular technology, studies will often include many different technologies (as seen in the aforementioned Australian examples). But another way to achieve diversity in renewable generation is through the spreading out of resources across vast geographical areas

Corresponding author address: Robert Huva, School of Earth Science, University of Melbourne VIC 3010, Australia
Email: robert.huva@gmail.com

(for instance wind speed as seen in Archer and Jacobsen (2007)). By spreading out resources and exploiting the spatial decorrelation of variables like wind speed the exposure of an interconnected system to low output events can be minimised. In this paper we want to ascertain whether or not the NEM region is a sufficiently large enough an area to have demand met predominantly by non-dispatchable wind and solar. The atmospheric synoptic scale is therefore of particular concern as this is the scale that encompasses the day-to-day variability of variables like wind speed and solar irradiance across spatial scales from 100s-1000s of kilometres. More commonly visualised by the distribution of high and low pressure centres, the synoptic scale describes the continuity of weather systems that stretch over vast continental-scale distances. The synoptic scale also provides the link between fundamental large-scale atmospheric dynamics like the Hadley cell and pressure systems that affect local weather conditions (Sturman and Tapper 2005).

In order to understand the influence of the synoptic scale on renewable energy output it is important to identify common patterns at the synoptic scale. One method for classifying synoptic scale weather systems that has become increasingly popular in recent decades is the Self Organising Map (SOM). The seminal use of SOMs in synoptic climatology was by Hewitson and Crane (2002) (hereafter referred to as H&C). H&C used the SOM technique to categorise a gridded Mean Sea-Level Pressure (MSLP) data-set of the northeast United States into 35 archetypal pressure distributions. H&C found the SOM to be a very useful method for determining common synoptic regimes as it presented an array of pressure maps that span the data-space and thus a continuum of synoptic maps was produced rather than, say, a group of clusters that have less obvious relationships to one another. Since H&C the SOM technique has become increasingly popular in climatology; a field in which it is more common to find Principal Component based clustering techniques (Sheridan and Lee 2011).

In terms of the Australian region, there have been a small number of noteworthy studies that have utilised the SOM technique. For instance, Alexander et al. (2010) used the European Centre for Medium-Range Weather Forecasts product ERA-40 to produce a 20 member SOM of MSLP. Other notable studies using the SOM technique in the Australian region include Brown et al. (2010), which utilised a 20 member SOM of Australian MSLP to study rainfall tendencies, Hope et al. (2006), which used 20 member SOM of MSLP to investigate synoptic links to rainfall in southwest Western Australia and Nicholls et al. (2010), which implemented a 20 member SOM of Australian MSLP to study synoptic influences on Melbourne temperature variations.

In this study we analyse how the commonly occurring synoptic weather types influence potential renewable energy production across the participating states of the National Electricity Network (NEM) (Queensland, New South Wales, Australian Capital Territory, Victoria, Tasmania and South Australia). We do so by splitting the work into two parts, which are then compared. In the first part we optimally place wind and solar resources to meet the electrical demand of the NEM. In the second part we use a SOM to classify commonly occurring MSLP patterns, and then we determine which of the SOM nodes occurred more/less often with low/high energy output. While the SOM is an increasingly popular tool in climatology and there are studies that examine combinations of wind and solar for Australia there is yet to be a study that combines the two areas. Combining the SOM analysis with renewable energy simulations enables a far more in depth analysis of the large-scale resource variance/covariance than possible with maps of average output and/or the output from the renewable electricity network.

Data and Methods

Data

The data used in this paper come from two main sources, in accordance with the requirements for each of the two methods. The weather typing requires a long time period for training purposes and the energy model requires finer resolution data in order to match demand and to assist with site selection flexibility. As such, the Self Organising Map was trained using the MSLP from the European Centre for Medium-Range Weather Forecasts product ERA-Interim for the period 1989-2009, while the energy model was run using Australian Community Climate and Earth-System Simulator (ACCESS) output for the Australian region (ACCESS-R) for the 2010-2011 period. ERA-Interim is available back to 1979, but at the time of the study it was not. Despite this, the time period of ERA-Interim output used fulfils the brief for the weather typing because it spans many decades into the past--enabling the SOM algorithm to capture as many synoptic systems as possible in the training process. The ACCESS-R data fulfil the brief for the energy model because of higher resolution (both temporally and spatially), which provides greater flexibility in site selection and at hourly resolution is able to match the demand for

electricity, which varies each day at a higher rate than the 6-hourly ERA-Interim. The ERA-Interim 2010-2011 MSLP data are also utilised later in the paper to assign SOM types for the period simulated by the energy model.

Figure 1   Domains for the a) ACCESS-A data and b) ERA-Interim data. In a) and b) the shading indicates the grid points utilised in the study, while the vertical axes represent latitude and the horizontal axes longitude
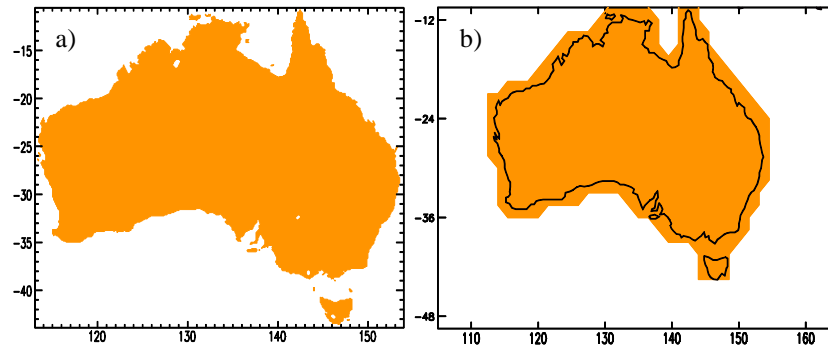
The ACCESS-R data are also trimmed to include only land areas of Australia (Figure 1a). The ACCESS-R data are hourly sampled and at 0.11 degrees longitude/latitude. The fields used in this article from the ACCESS-R model were the model level wind speed and the Downward Shortwave Radiation (DSR) at the surface. The demand data used in the energy model come from the Australian Electricity Market Operator and are half-hourly resolved. The data for each NEM region are aggregated and the NEM-wide demand for electricity utilised at an hourly step. The aggregation of demand follows the copper-plate approach whereby the demand for electricity in the NEM can be instantaneously met by the generated output without considering where that generation is located. The copper-plate plate approach is a best case scenario and in reality there would need to be power flow considerations.

The ERA-Interim data were sampled for the Australian region using the domain covering (10.5°S, 105°E) to (49.5°S, 165°E) (Figure 1b). The ERA-Interim data have spatial resolution 1.5 degrees longitude/latitude, temporally sampled every 6 hours. For the training of the SOM the ERA-Interim data had the ocean MSLP variability filtered out. Further analysis, not presented here, shows that a SOM of just continental MSLP data is much more accurate at mapping back onto the original data. This is due to transient low pressure systems to the south of Australia, which are a large source of error when mapping the SOM back on to the data. More matches pass the filtering process (outlined below) when matching just the pressure distributions over the continent. Further, this study is focused on the variability over the Australian continent as this is the region of interest for renewable energy installations.

Methods

Creating and filtering the Self Organising Map

The training of the SOM in the current study occurred in two phases, following the methodology of Kohonen et al. (1995) and using the ERA-Interim MSLP for 1989-2009. The first phase of training takes the SOM space (initially randomised) and shows the data once, altering the SOM nodes to look more like the MSLP data. The second phase utilises the SOM space from the end of the first phase. The SOM is shown the data again in the second phase, but several times over and with a decreasing amount of alteration to the SOM space with each showing. The alteration of the SOM is controlled by radius and alpha parameters, which in turn control the rate of decay of a Gaussian function centred on the closest matching SOM node for each time step in the data (see Kohonen et al. (1995) for a more rigorous description of the algorithm). After training the SOM it is then possible to go through the original data and assign the closest looking SOM node (known as the Best Matching Unit/SOM node (BMU)) to each member of the data set (determined using Euclidean distance). Following the mapping of the SOM nodes back on to the original data the filtering process outlined in Huva et al. (2015) was also undertaken. The process of checking the BMUs ensures that the purpose of the current study--to determine the synoptic influences on wind and solar output--is not undermined by falsely assigning SOM nodes to conditions from the original data-set.

The energy model and optimisation

Renewable Energy (RE) studies often utilise optimisation techniques when trying to solve for the optimum combination of resources to meet a required goal--this might be increasing the penetration of renewable resources or reducing carbon emissions from the electricity sector. Optimisation techniques offer the advantage of being able to incorporate computer resources to solve complicated and multi-faceted problems in a relatively short amount of time. As such, the use of optimisation techniques for RE research has become increasingly popular in recent years (Baños et al. 2011). Common among most RE studies, and the field of optimisation in general, is the use of a cost function as the object for minimising.

In this paper we utilise a Genetic Algorithm to minimise a cost function. The implementation of the Genetic Algorithm in this article is outlined in Rayner (2004). In the current study the cost function is comprised of costs associated with building and maintaining the installed capacity of each resource. The cost of wind and solar is designed to follow an economies of scale approach. In the economies of scale approach the cost of using a location is the sum of an install cost plus an incremental cost for each new turbine/solar farm added to a site. The cost per new turbine/solar farm is high for small volumes and asymptotes towards the manufacturing cost (Capex in Table 1). It is assumed that existing hydro capacity is available and as such the hydro capital expenditure (Capex) is zero, while the cost of utilising gas is intentionally large to discourage its use. Specifically, the cost of gas is the sum of the gas output (MW) multiplied by a linear combination of pre-defined fuel and carbon prices. This total is then further multiplied by a factor of 10 to account for the fact that fuel costs are the main source of expenditure for gas-fired power plants and we only simulate 2 years out of a power plant lifetime of roughly 20 years. Gas also incurs the capital expenditure costs (maximum output multiplied by Capex from Table 1).

The costs for each technology define the order in which the technologies are dispatched. The available technologies are onshore wind, large-scale photovoltaics, pumped hydro and gas-fired back-up. The back-up hydro and gas models utilised are originally outlined in Huva et al. (2012). The energy model requires that demand is met by the mixture of technologies and the total cost will vary based on the amount that each resource is deployed. The energy model in this article balances the output of each given technology, combines the costs involved into a single dollar amount and then informs the Genetic Algorithm of the total cost following each evolution of the solution space.

Energy model site selection

It is not necessary (and infeasible) to consider every possible gridpoint that contains meteorological data in the energy system network optimisation. Decorrelation lengths exist in the atmosphere for most fields (in particular the wind field, but also the solar field) and indicate that adjacent locations have significantly similar time series. Based on a decorrelation analysis (not shown) we consider gridpoints for inclusion in the RE network that are spaced apart by 120 km for the wind field, and 250 km for the solar field. The locations used in this article for solar and wind data are shown in Figure 2a and Figure 2b, respectively, which show the regular grid. Note that locations that would not be available to RE (i.e. due to coincidence with urban areas, national parks or waterways) are not included. This exclusion is determined using a Geoscience Australia GIS data-base. The availability of sites was limited to the NEM region as this was the source of the demand for electricity in the model.

Figure 2   Regular grid of locations utilised in the energy model optimisation for a) DSR and b) wind speed
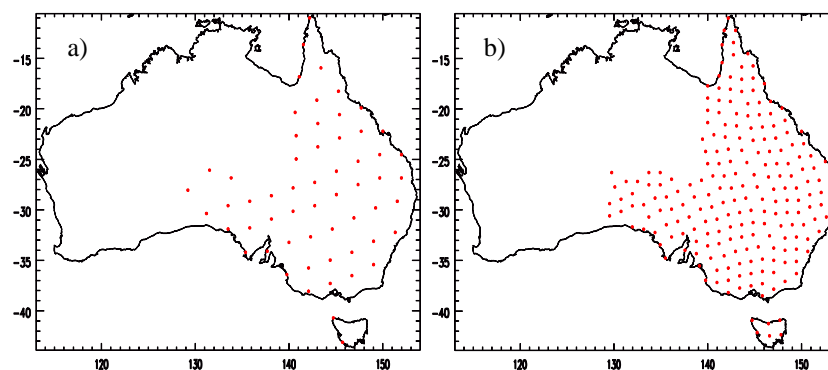
Wind speed at model levels was interpolated to 80 m above ground using a cubic spline in order to obtain wind speeds that were at the approximate hub height of a wind turbine. The 80 m wind speed time series at each location from Figure 2b was then converted to power using the conversion curve in Figure 3. The power curve is based on observations of wind speed and power output from GE 2.5 MW turbines. The conversion uses two quadratic lines of best fit (as well as the zero line and 2.5 MW rated power output line) to approximate the average relationship between power output and turbine-height wind speed. Currently, most land-based turbines have a rating of between 1.5 MW and 3.5 MW (REN21 2013) and future cost reductions will likely dictate larger amounts of 3.5 MW+ capacity turbines being installed. Typically the wind speed characteristics at each site dictate the turbine rating, but this was not optimised in the article. The 2.5 MW turbine was used to give an indicative power output for each site in Figure 2b. Each location from Figure 2a had its DSR data converted to a percentage of maximum, instead of power. The maximum was taken as the highest DSR value in the ACCESS-R data ($1184.3 \ W/m^2$). This approach for DSR gave a measure of solar availability without a predetermination as to which type of solar technology to use. We assume that any solar installation would be operating at 100 % when exposed to $1184.3 \ W/m^2$.

Figure 3   Power conversion curve for a GE 2.5 MW wind turbine used to convert wind speed values to wind power. Curve is constructed using two quadratics (upper and lower) along with the constant values at 0 MW and 2.5 MW
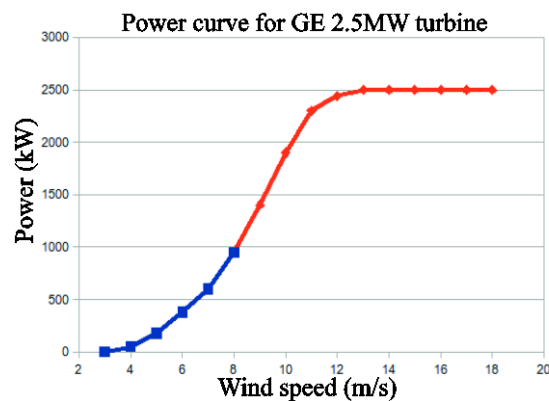
Results

The following results section is divided into two sections that present the results from a simple optimisation of Renewable Energy (RE) resources for the NEM, followed by the presentation of the SOM and the SOM nodes that co-occur with either high or low RE.

Optimisation of the NEM

Figure 4 illustrates the least-cost configuration of wind and solar capacity that, along with hydro and gas reserves, meets demand using the costs outlined in Table 1and following a 100-member, 10,000 iteration search of the solution space. An optimised solution was the minimum value from the 10,000 iterations, and where 10,000 iterations was seen to be enough to converge on an effectively un-changing cost function value. The resulting time series of wind plus solar, gas and hydro is shown in Figure 5.

It should be noted that each location seen in Figure 2a and Figure 2b had a penalty applied based on its distance to the nearest capital city of $1M/km (Table 1). The capital cost utilised was in accordance with Humpert (2012) who suggested that high-voltage direct current cabling costs approximately $1M/km to build. The penalty encourages the use of locations closer to the demand centres, but does not take into consideration the limitations of power flow through transmission lines.

Table 1   Capital expenditure (Capex) values and gas-fired back-up penalties used in the optimisation of the NEM region

Capex:	Cost ($M/MW):	Gas Params:	Value:
Wind	1.2	Carbon Price	$80/Tonne
Solar	1	Fuel Price	$25/MWh
Hydro	0		
Gas	1		
Transmission Penalty	1		

Figure 4   Distribution of installed capacity for the optimised network. Blue squares represent wind capacity relative in size to the largest square (11 GW). The red triangle represents solar capacity for the 13.5 GW station
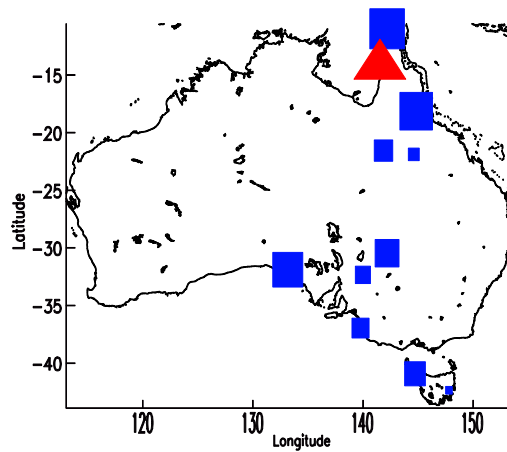
Figure 5   Cumulative time series output for the optimised network (hydro plotted on top of gas, which is on top of wind and then solar output). Output is daily averaged and hydro output above demand (black curve) indicates water pumping uphill while the reverse (release of water downhill) is true for hydro below the demand curve
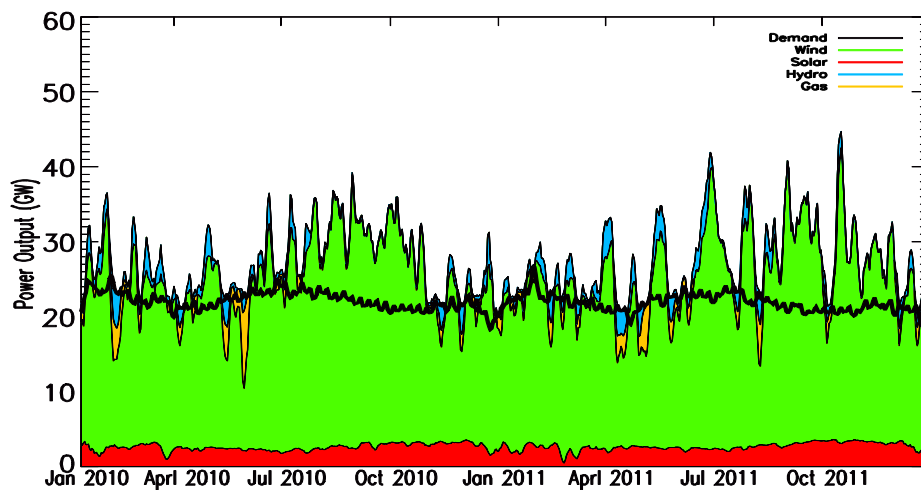
As can be seen from Figure 5 there are still many moments where an optimised combination of wind and solar alone cannot meet the NEM demand for electricity—even at daily averaged values. This implies that a cost-effective high penetration renewable energy system will need to have some dispatchable power generation, such as from geothermal, biomass, or large increases in the amount of hydropower. It also raises the question as to what the large-scale synoptic influences are at these times of low output, and if any of these low RE episodes have significant links to particular types of weather events.

Table 2   Resource statistics for the NEM optimisation. Capacity Factor is the total output as a percentage of the output had the resource been operating at capacity for all times

Resource:	Capacity (GW):	Capacity Factor (%):
Wind	67	35
Solar	13	20
Hydro	5	26
Gas	20	5

Creating and filtering the continental SOM

By testing SOMs of various sizes it was determine that the appropriate number of nodes was 30 (using the technique described in Huva et al. 2015 to balance data representation and aesthetics). The SOM with 30 nodes that had the closest match to the original 1989-2009 training data had initial alpha of 0.5 and is shown in Figure 6.

As can be seen from Figure 6 there is a clearly defined continuum of synoptic classifications that range from low-pressure intrusions on the left hand side of the figure to high pressure intrusions on the right hand side (consistent with previous studies including Alexander et al. (2010)). Transitional phases between episodes of high and low pressure dominance are also visible in Figure 6, while it is possible to see the 'traditional' west-to-east cycle between successive high pressure systems if one traces out the SOM perimeter in an anticlockwise fashion.

Once created the next step was to map the 30 SOM nodes onto the 2010-2011 ERA-Interim MSLP data. Each time step from 2010-2011 was assigned a SOM node based on Euclidean distance and then the filtering process outline in Huva et al. (2015) was employed (using the (20 hPa, 5 %, 4 hPa) set of conditions). In total there were 177 false assignments out of 2,920 ERA-Interim time steps for 2010-2011.

Analysis of low RE events

The identification of a low RE event is described in the following process:

- Any ACCESS-R time step that had a combined RE output that was more than 20 % below demand was defined to be a low RE time step.
- An event was deemed to be a collection of consecutive low RE time steps. Except where:
    - The next low RE time step is within six hours of the previous low RE time step

  OR

    - A time step is within six hours of the nearest low RE time step and only just failed the original criterion of being more than 20 % below demand. The definition of only just failing was deemed to be a time step where the combined RE output was more than 15 % below demand.

The 20% below threshold was relaxed to 15 % in some instances in order to increase the continuity of events. 20 % below demand was seen as an appropriate figure, but should (for example) a time step only just fail this criterion and was a critical time step for continuing a new event or not, it was also included. By relaxing the threshold and maximising the continuity of events there were then more events considered, which in turn aided later statistical analysis.

Figure 6 SOM nodes of ERA-Interim 1989-2009 continental MSLP data for the Australian region. Horizontal axes are in units of degrees longitude and vertical axes are in units of degrees latitude
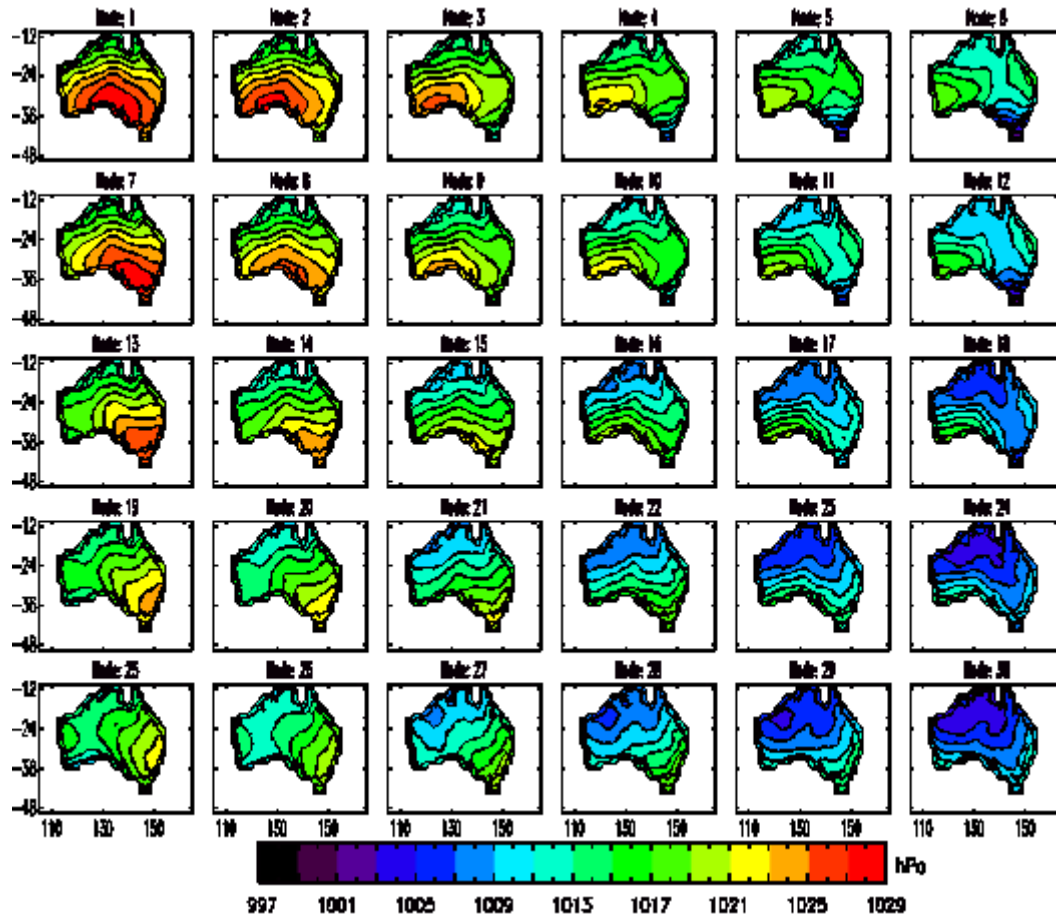

Figure 7 Percentage occurrence of very low (worst of the worst) RE time steps that are associated with each SOM node from Figure 6. Colours and italics represent significant associations and where red indicates significantly high while green represents significantly low. Significance is measured at the 5 % level using a two-tailed Monte-Carlo simulation and darker grey indicates larger values

	1	2	3	4	5	6
1	0.7	0.8	1.8	*0.6*	2.1	0.1
2	3.1	6.5	*11.2*	6.5	4.3	2.1
3	2.1	4.0	5.7	5.5	1.8	2.1
4	1.0	1.8	3.2	4.0	3.7	1.8
5	*0.0*	1.9	3.2	2.9	6.9	8.5

Figure 7 shows the relationship between the SOM nodes and very low RE time steps from the optimised network (expressed as a percentage of very low RE time steps that co-occur with the SOM nodes). Very low RE was deemed to be the lowest 20 % of low RE time steps. Plotting of just the association between low RE and the SOM showed some significant

relationships (not shown), however plotting of the worst 20 % (Figure 7) showed more clearly the regions of the SOM/synoptic types that are problematic, as well as those regions that are not problematic.

Significance testing was undertaken via the bootstrapping/Monte-Carlo approach (Chapter 5.3.3 from Wilks (2011)). Similar to that of Uotila et al. (2007) the occurrence of SOM nodes in time was randomised in order to assess the chance that such relationships between low RE and SOM node were possible, at some significance level, by random. However, the randomising was also weighted by the SOM node transition probabilities for the 2010-2011 period, which ensured the autocorrelation in the MSLP field was conserved. In total there were 10,000 time series where the occurrence of SOM nodes was randomised. The frequency distribution from the 10,000 member served as the comparison for significance testing. If the measured percentage occurrence was in either tail of the distribution (2.5 % of the distribution in each tail) the actual occurrence was said to be significant at the 5 % level.

As can be seen from Figure 7 there were some SOM nodes that had very low percentages or never co-occurred with very low RE for the NEM simulation. Node 25 significantly never co-occurred with the lowest RE output. Node 9 had the highest and most significant relationship with very low RE output. There was a region of the SOM surrounding node 9 (nodes 8-10 and 14-16) that represented almost 40 % of all of the very low RE time steps. Given the smooth nature of the SOM these nodes represent similar MSLP distributions and therefore represent a sub-set of similar synoptic regimes from within the SOM that were associated with nearly half of all very low RE time steps. Another notable association seen in Figure 7 is that of node 30, which at 8.5 % of the lowest RE time steps was also a relatively high amount. Node 30 is a summertime node and is also quite far removed from the significant sub-set of nodes (8-10 and 14-16).

Analysis of nodes 9 and 30

This section analyses nodes 9 and 30 and their relationship to very low renewable energy output. In particular, any meteorological reasons for why these synoptic regimes were problematic for the optimised simulation. Figure 8 shows the MSLP patterns when these nodes were said to occur with very low RE. The composite of very low RE for node 9 is characterised by a relatively weak centre of high pressure just off the coast of Western Australia and occurred predominantly in late Austral Autumn (May- June).

Figure 8   Composite ERA-Interim MSLP for (a) SOM node 9 and (b) SOM node 30 for time steps that co-occur with very low RE output for the 2010-2011 period
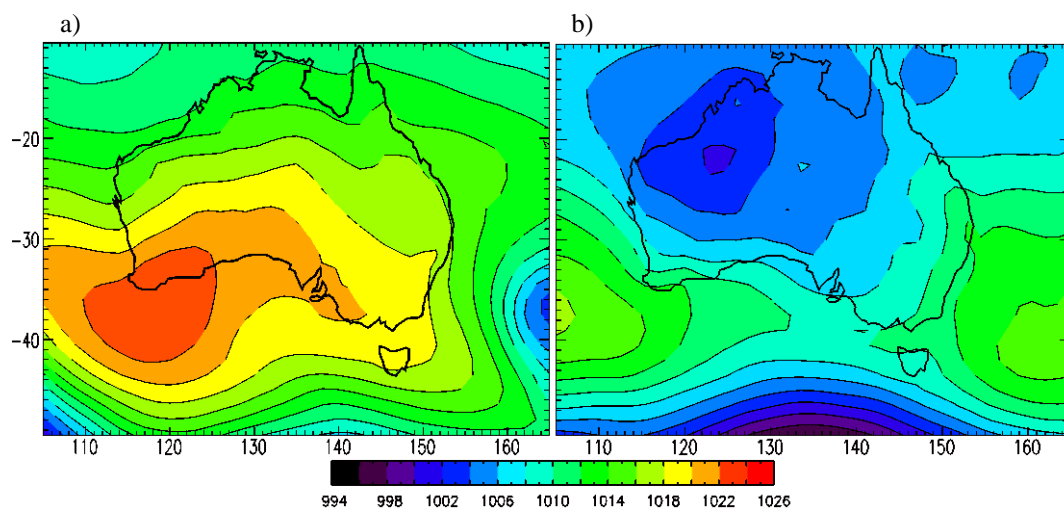
Node 30 is characterised by lower pressure over Western Australia (Figure 8b) and occurred predominantly in late Austral Summer (Feb-March). Node 30 could be considered as a continental heat low, which also occurs in summertime. Node 30, as per node 9, was also characterised by low pressure gradients across the Austral domain. Both nodes 9 and 30 were, as a consequence of their small pressure gradients, both associated with low average wind speeds across the NEM region (Fig-

Huva et al. Synoptic types for renewable energy

351

ure 9a and Figure 9b). Stippling in Figure 9 shows that much of the NEM region experienced average wind speeds below 4 m/s (2 % of capacity) when the low RE output versions of nodes 9 and 30 occurred. Low wind speeds are detrimental to the optimised network due to the reliance on wind speed to meet demand. However, both nodes were not particularly biased towards low RE output on the whole. Figure 10a and Figure 10b indicate that when analysing all occurrences of nodes 9 and 30 there was no significant bias towards low average output, only that these nodes have the potential to produce very low RE output for the optimised network presented earlier.

Figure 9   80 m wind speed anomaly plots for the occurrences of a) SOM node 9 and b) SOM node 30 that co-occur with very low RE. Anomaly is node average minus the 2010-2011 average and hatching indicates locations that have a 2010-2011 average wind speed of less than 4 m/s (or 2 % of capacity)
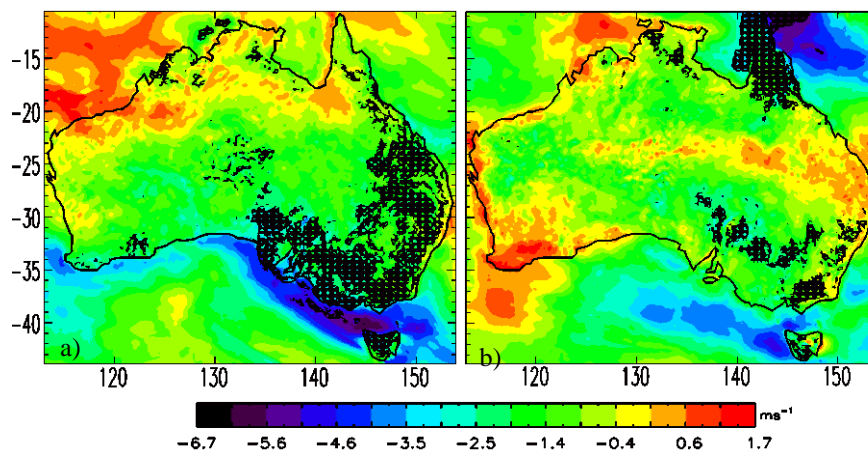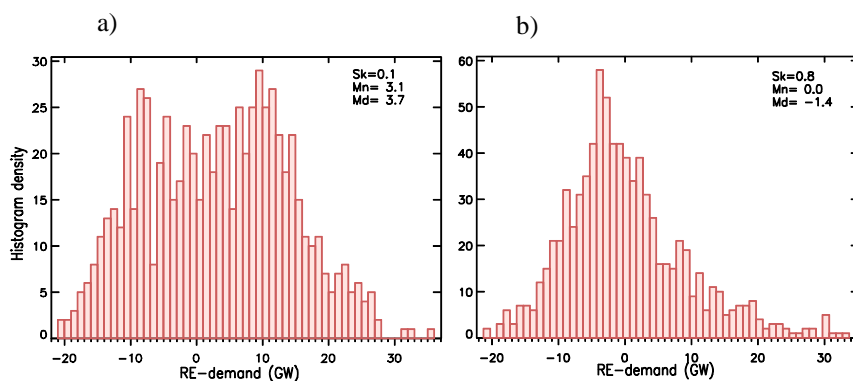

Figure 10   Distribution of RE - demand when a) SOM node 9 and b) SOM node 30 occurred in the optimised energy simulation. Histogram density indicates the number of hours in the simulation where the SOM nodes are either over or under producing RE in comparison to demand. Distribution characteristics appear top-right where Sk is Skewness, Mn is Mean and Md is Median

Analysis of node 25

Contrary to nodes 9 and 30, node 25 was significantly never associated with very low RE output. In fact the distribution of RE – demand for node 25 indicates that this node had a very clear bias towards oversupply (Figure 11). The MSLP distribution for node 25 shows low pressure intruding into southern Australia as well as much stronger pressure gradients throughout the NEM region when compared to nodes 9 and 30 (Figure 12). In fact, only 27 hours out of the total of 828 for node 25 were associated with undersupply from RE.

Figure 11   As per Figure 10, except for node 25
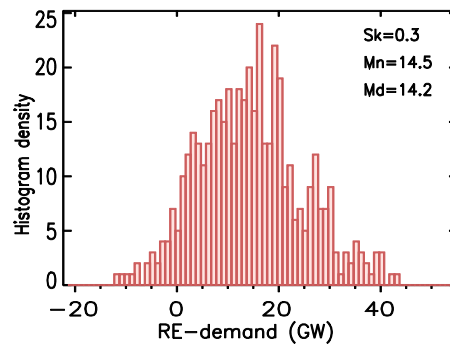
Figure 12   Composite ERA-Interim MSLP from 1989-2009 when SOM node 25 is said to occur
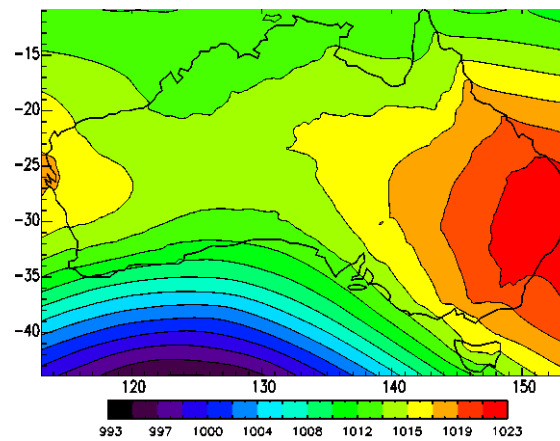
Comparing 2010-2011 with 1989-2009

Given the relatively strong La Nina pattern that prevailed during the 2010-2011 period it raises the question as to whether or not this period, which is used to form the optimised network, is a biased representation of the meteorological conditions for eastern Australia. Some of the SOM nodes show altered frequencies during the 2010-2011 period, while the DSR and wind speed fields show a decrease in eastern Australia when compared to the mean of 1989-2009. Figure 13 and Figure 14 show the percentage change in DSR and 80 m wind speed for the 2010-2011 period in comparison to the 1989-2009 period using the ERA-Interim data. Figure 13b shows a drop-off in short-wave radiation reaching the surface for 2010-2011 (6-10 % in a large section of the eastern coastline). This decrease concords well with an increase in rainfall for those years. The change in 80 m wind speed was less pronounced with small decreases for much of the southern states, and with the largest decrease occurring near Adelaide at 6.3 %. However, given the cubic relationship between wind speed and power this change would have been more significant for power output.

Figure 13   In a) the average for the 2010-2011 ERA-Interim of DSR and in b) the percentage difference between ERA-Interim DSR for the 2010-2011 period when compared to the 1989-2009 period
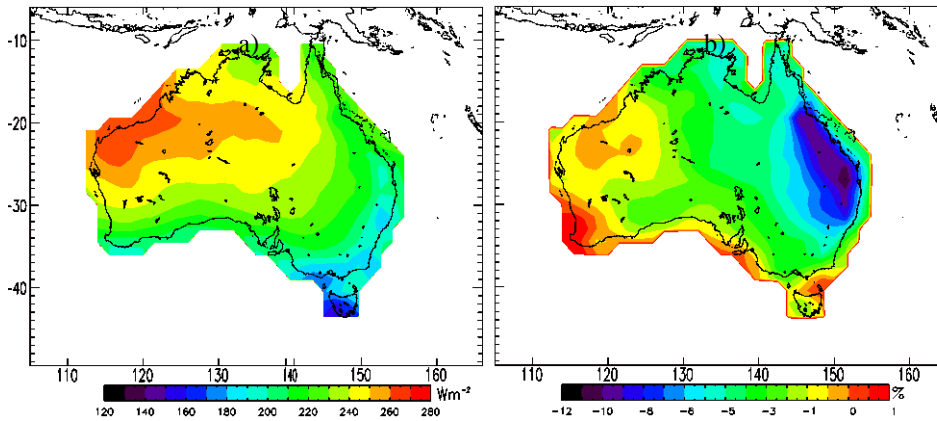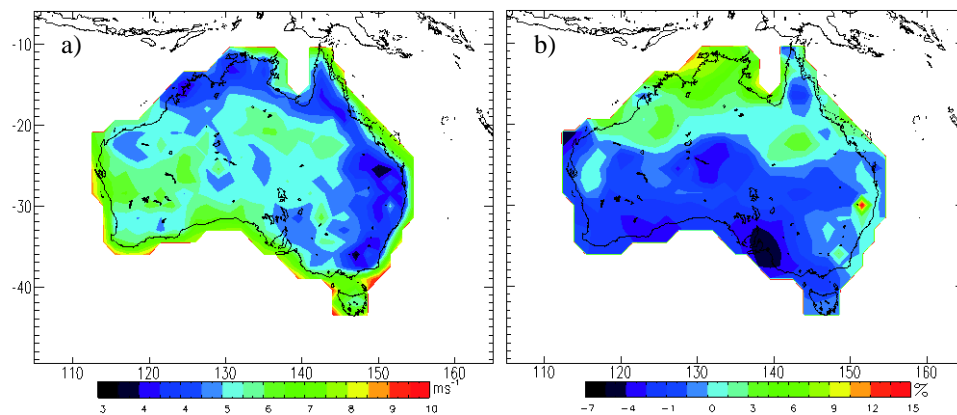

Figure 14   As per Figure 13, except for 80m interpolated ERA-Interim wind speed and the relative change (%) between 2010-2011 and 1989-2009

In terms of the occurrence of the SOM nodes during 2010-2011, in particular the significant/notable nodes (9, 30 and 25), there is a large change in the occurrence of node 30 when compared to the 1989-2009 period (Figure 15). For node 30 the 1989-2009 mean is 36.85 occurrences/year with a standard deviation of 15.7. However, in 2011 there were 91 occurrences of node 30, which is 3.5 standard deviations from the 1989-2009 mean. While node 30 did not have a particular bias towards low RE output, the prevalence of node 30 in combination with the lower averaged wind speed and solar irradiance indicates that the 2010-2011 was a relatively difficult period to optimise. For the other nodes of interest (9 and 25) there was no discernible shift in the occurrence when compared to the 1989-2009 period (not shown).

Figure 15 The annual total occurrence of SOM node 30 for the 1989-2011 period
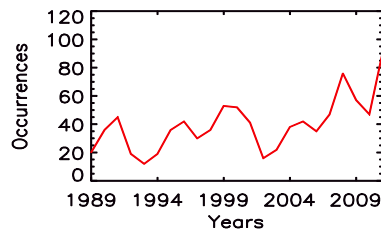
Discussion/Conclusion

After building an energy model for the NEM region and maximising the contribution from wind and solar (RE) it was shown that two synoptic weather types were significantly associated with very low output from the RE resources, while one other synoptic type was shown to have very clear biases towards oversupply. Both the of the very low RE weather types were shown to produce average wind speeds across much of the NEM region below 4 m/s, or 2 % of capacity. Average wind speed maps for the very low RE weather types also suggested that any optimised network for the NEM that relied on wind power would have struggled to produce enough power to meet demand during their occurrence. Conversely, one weather type that never occurred with very low RE had much larger pressure gradients associated with low pressure systems to the south and averaged over 14 GW of oversupply (RE output above demand). All three weather types were created via a Self-Organising Map and thus represent relatively common pressure distributions. The results therefore indicate challenges for a future NEM that is heavily reliant on wind energy. If the aim is to have a NEM reliant on only renewable resources what the very low RE weather types also show is a need for integrating non-weather-dependent renewable resources and/or storage. It is entirely possible that the very low RE weather patterns are quite predictable and given enough warning a NEM that has enough storage or dispatchable renewable generation capacity (i.e. geothermal, biomass or more hydro) could deal with the wide-spread low wind speeds. Finally, it was shown that in comparison to the long-term mean the period that was available for the optimisation (2010-2011) was a challenging period for RE. Below average wind speed and solar irradiance for 2010-2011 also indicates that the back-up resources utilised in the optimal configuration are likely to be enough for other years with better resources, as well. Future work should include an investigation into such large-scale interannual variability in renewable resources for the NEM region.

Acknowledgements

References

AEMO. 2013. *100 per cent renewables study modelling outcomes*, Australian Electricity Market Operator report, Melbourne, 111pp

Alexander, L. V., Uotila, P., Nicholls, N. and Lynch, A. 2010. A New Daily Pressure Dataset for Australia and Its Application to the Assessment of Changes in Synoptic Patterns during the Last Century, *J. Clim.*, 23, 1111-1126, doi:10.1175/2009jcli2972.1

Archer, C. L. and Jacobson, M. Z. 2007. Supplying baseload power and reducing transmission requirements by interconnecting wind farms, *J. Appl. Meteorol. Clim*, 46, 1701–1717, doi:10.1175/2007JAMC1538.1

Baños, R., Manzano-Agugliaro, F., Montoya, F., Gil, C., Alcayde, A. and Gómez, J. 2011. Optimization methods applied to renewable and sustainable energy: A review, *Renew. and Sus. Energy Rev.*, 15, 1753-1766, doi:10.1016/j.rser.2010.12.008

Brown, J. R., Jakob, C. and Haynes, J. M. 2010. An evaluation of rainfall frequency and intensity over the Australian region in a global climate model, *J. Clim.*, 23, 6504-6525, doi:10.1175/2010JCLI3571.1

Elliston, B., MacGill, I. and Diesendorf, M. 2013. Least cost 100% renewable electricity scenarios in the Australian National Electricity Market, *Energy Policy*, 59, 270-282, doi:10.1016/j.enpol.2013.03.038

Hewitson, B. C. and Crane, R. G. 2002. Self-organizing maps: applications to synoptic climatology, *Clim. Res.*, 22, 13-26

Hope, P. K., Drosdowsky, W. and Nicholls N. 2006. Shifts in the synoptic systems influencing southwest Western Australia, *Clim. Dyn.*, 26, 751-764, doi:10.1007/s00382-006-0115-y

Humpert, C. 2012. Long distance transmission systems for the future electricity supply--Analysis of possibilities and restrictions, *Energy*, 48, 278-283, doi:10.1016/j.energy.2012.06.018

Huva, R., Dargaville, R. and Caine, S. 2012. Prototype large-scale renewable energy system optimisation for Victoria, Australia, *Energy*, 41, 326-334, doi:10.1016/j.energy.2012.03.009

Huva, R., Dargaville, R., and Rayner, P. 2015. The impact of filtering self-organizing maps: a case study with Australian pressure and rainfall, *Int. J. Clim.*, 35, 624-633, doi:10.1002/joc.4008

Kohonen, T., Hynninen, J., Kangas, J. and Laaksonen, J. 1995. *SOM_PAK: The Self-Organising Map Program Package*. Tech. rep., 27 pp., Rakentajanaukio

Nicholls, N., Uotila, P. and Alexander, L. 2010. Synoptic influences on seasonal, interannual and decadal temperature variations in Melbourne, Australia. *Int. J. Clim.*, 30, 1372-1381, doi:10.1002/joc.1965

Rayner, P. J. 2004. Optimizing CO2 observing networks in the presence of model error: results from TransCom 3, *Atmos. Chem. Phys. Discuss.*, 4, 413-421, doi:10.5194/acpd-3-5185-2003

REN21. 2013. *Renewables 2013 Global Status Report*. Tech. rep., 178 pp, doi: ISBN 978-3-9815934-0-2

Sheridan, S. C. and Lee, C. C. 2011. The self-organizing map in synoptic climatological research, *Prog. Phys. Geogr.*, 35, 109-119, doi: 10.1177/0309133310397582

Sturman, A. P. and Tapper, N. J. 2005. *The weather and climate of Australia and New Zealand*, 2nd ed., Oxford University Press, South Melbourne, 541 pp

Verdon-Kidd, D. C. and Kiem, A. S. 2009. On the relationship between large-scale climate modes and regional synoptic patterns that drive Victorian rainfall, *Hydrol. Earth Sys. Sci.*, 13, 467-479

Wilks, D. S. 2011. *Statistical Methods in the Atmospheric Sciences*, 3rd ed., Elsevier, Oxford, 676 pp.

Wright, M. and Hearps, P. 2010. *Zero Carbon Australia Stationary Energy Plan*, Beyond Zero Emissions, Melbourne, 194 pp.